Double folding model calculation applied to fusion reactions[*]

ZHANG Gao-Long(张高龙)[1)]   LE Xiao-Yun(乐小云)

(Department of Physics, School of Sciences, Beijing University of Aeronautics & Astronautics, Beijing 100083, China)

Abstract The interaction potential between a spherical and a deformed nucleus is calculated within the double-folding model for deformed nuclei. We solve the double folding potential numerically by using the truncated multipole expansion method. The shape, separation and orientation dependence of the interaction potential, fusion cross section and barrier distribution of the system ^{16}O+^{154}Sm are investigated by considering the quadrupole and hexadecapole deformations of ^{154}Sm. It is shown that the height and the position of the barrier depend strongly on the deformation and the orientation angles of the deformed nucleus. These are quite important quantities for heavy-ion fusion reactions, and hence produce great effects on the fusion cross section and barrier distribution.

Key words heavy-ion fusion reaction, double folding model, deformation, barrier distribution

PACS 25.70.Jj, 24.10.-i

1   Introduction

Heavy-ion fusion reactions involving deformed nuclei are an important topic of research in nuclear physics[1, 2]. Recently, particular interest has been paid to the effects of nuclear deformation on the production and decay of superheavy nuclei. This is because reasonable predictions of production cross sections and α-decay half-lives of superheavy nuclei require the knowledge of the nuclear potentials. The nuclear potentials between deformed interacting nuclei are essentially important in describing these reactions and decay processes. Therefore, fusion reactions between heavy nuclei with static and dynamic deformations have re-attracted much attention up to date. It is also important to explore the situation where one of the interacting pair of nuclei is spherical and the other one deformed.

The double folding model is commonly used to calculate the optical potential in elastic scattering[3]. If it is used for the calculation of the interaction potential in a fusion reaction, the barrier height and position can be obtained. Then the fusion cross section

and barrier distribution can easily be obtained. The basic input into the folding calculation is the nuclear density of both of the colliding nuclei. The folding of two spherically symmetric distributions can easily be calculated by using the double folding model. However, if one or both of the nuclei have a deformed density distribution, it is much more difficult to simplify the six-dimensional integral and reduce it to fewer dimensions. In this case, one usually simplifies the folding model by using the truncated multipole expansion method[4]. In this letter, we limit ourselves to the interaction potentials between a deformed target and a spherical projectile (see Fig. 1). The double folding potentials are calculated numerically by using the above mentioned method. We consider an axially symmetric shape for the multipole expansion of the target nuclear distribution. The system ^{16}O+^{154}Sm is chosen to study the deformation and orientation dependence of the interaction potentials, fusion cross sections and barrier distribution within the double folding model. Both quadrupole and hexadecapole deformations are included for the ^{154}Sm nucleus.

2 The interaction between a spherical and a deformed nucleus in the double folding model

In the double folding model the nuclear potential is calculated as

$$V_N(r) = \iint \rho_P(r_1)v\big(s = |\boldsymbol{R}+\boldsymbol{r}_2-\boldsymbol{r}_1|\big)\rho_T(r_2)\mathrm{d}\boldsymbol{r}_1\mathrm{d}\boldsymbol{r}_2, \tag{1}$$

where v is the NN interaction between two nucleons. $\rho_P(r_1)$ and $\rho_T(r_2)$ are the matter density distributions of the projectile (P) and target (T) nuclear ground states, normalized as:

$$\int \rho_i(\boldsymbol{r}_i)\mathrm{d}\boldsymbol{r}_i = A_i. \tag{2}$$

The vector $\boldsymbol{s} = \boldsymbol{R}+\boldsymbol{r}_2-\boldsymbol{r}_1$ corresponds to the distance between two specified interacting points of the projectile and target, whose radius vectors are $\boldsymbol{r}_1$ and $\boldsymbol{r}_2$, respectively. $\boldsymbol{R}$ denotes the vector between the center of mass of the two nuclei. θ is the relative orientation angle of the target nucleus symmetry axis measured with respect to the separation vector $\boldsymbol{R}$. This geometry is illustrated in Fig. 1.
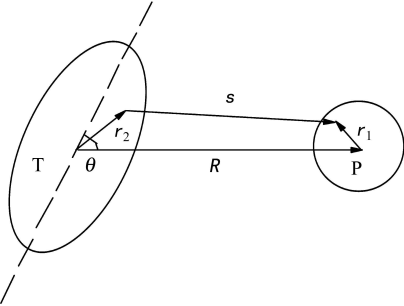
Fig. 1.   The coordinate system used in the double folding model.

The densities of deformed nuclei have the form

$$\rho(r,\theta) = \frac{\rho_0}{1+\exp[(r-R(\theta))/a]}, \tag{3}$$

where $R(\theta)$ is the half density radius

$$R(\theta) = R_0[1+\beta_2 Y_{20}(\theta)+\beta_4 Y_{40}(\theta)]. \tag{4}$$

The multipole expansion of the deformed nuclear density distribution for an axially symmetric shape, limiting the deformations to quadrupole and hexadecapole cases, has the form

$$\rho(r,\theta) = \sum_{l=0,2,4} \rho_l(r)Y_{l0}(\theta). \tag{5}$$

As NN interaction we used the well-known M3Y-Reid zero-range interaction[5]. The multipole components of the intrinsic form factor are given by[6]

$$\tilde{\rho}_T^{(l)}(k) = \int_0^{r_{\max}} \mathrm{d}r r^2 \rho_l(r)j_l(kr). \tag{6}$$

The double folding potential is obtained by the summation over the different multipole components[7].

$$V_N(R,\theta) = \sum_{l=0,2,4} V_N^l(R,\theta), \tag{7}$$

with[8]

$$V_N^l(R,\theta) = \frac{2}{\pi}\left[\frac{2l+1}{4\pi}\right]^{1/2}\int_0^{k_{\max}} \mathrm{d}kk^2 j_l(kR)\times$$
$$\tilde{\rho}_P(k)\tilde{\rho}_T^{(l)}(k)\tilde{v}(k)P_l(\cos\theta), \tag{8}$$

where $\tilde{\rho}_P(k)$ and $\tilde{v}(k)$ are the Fourier transforms of the density distribution of the spherical projectile and the M3Y-Reid zero-range NN interaction, respectively.

The Coulomb potential is calculated with[9]

$$V_C(R) = 2\pi e^2 \int_0^\infty j_0(kR)\hat{\rho}_P(k)\hat{\rho}_T(k)\mathrm{d}k, \tag{9}$$

where $\hat{\rho}_P(k)$ and $\hat{\rho}_T(k)$ are the Fourier transforms of the spherically symmetric charge densities of projectile and target.

3 The system $^{16}O+^{154}Sm$

The system $^{16}O+^{154}Sm$ is chosen to calculate the nuclear and Coulomb potentials. We use electron scattering data for ^{16}O and ^{154}Sm[10]. A two-parameter Fermi shape is used for ^{16}O with R_0=2.6 fm and a=0.45 fm,

$$\rho_P(r) = \frac{\rho_0}{1+\exp((r-R_0)/a)}. \tag{10}$$

For ^{154}Sm, β_2=0.311, β_4=0.087, R_0=5.9387 fm and a=0.5223 fm is used[11]. The density distributions obtained by using the multipole expansion method for l=0, 2, 4 are shown in Fig. 2.

Using the above formula, the interaction potentials between ^{16}O and ^{154}Sm are shown for the orientation angles $\theta = 0°$ and $\theta = 90°$ in Fig. 3. We see that the barrier height is much lower at $\theta = 0°$ than at $\theta=90°$. This is so because there is a larger overlap at $\theta=0°$ and the nuclear potential for $\theta=0°$ is much more attractive than that for $\theta=90°$. Simultaneously we evaluate the barrier heights and positions of the system without deformation and for hexadecapole deformations with β_4=0 and β_4=0.087 for the target nucleus ^{154}Sm at different orientation angles. The results are shown in Fig. 4. One can see that the barrier heights and positions change with the orientation angles and deformations of the target nucleus. The barrier heights increase and the barrier positions decrease with increasing orientation angles. Fig. 4 shows also the influence of different values of the hexadecapole deformations on the behaviour of the barrier heights and positions.
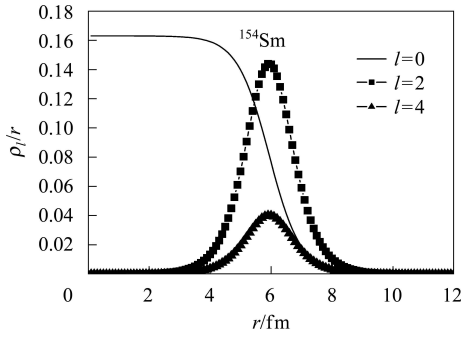
Fig. 2. The radial density distributions for ^{154}Sm at $l=0, 2, 4$.
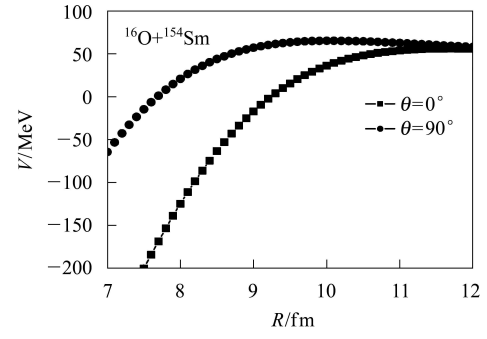
Fig. 3. The interaction potentials of the system ^{16}O$+^{154}$Sm at the orientation angles $\theta=0°$ and $\theta=90°$.
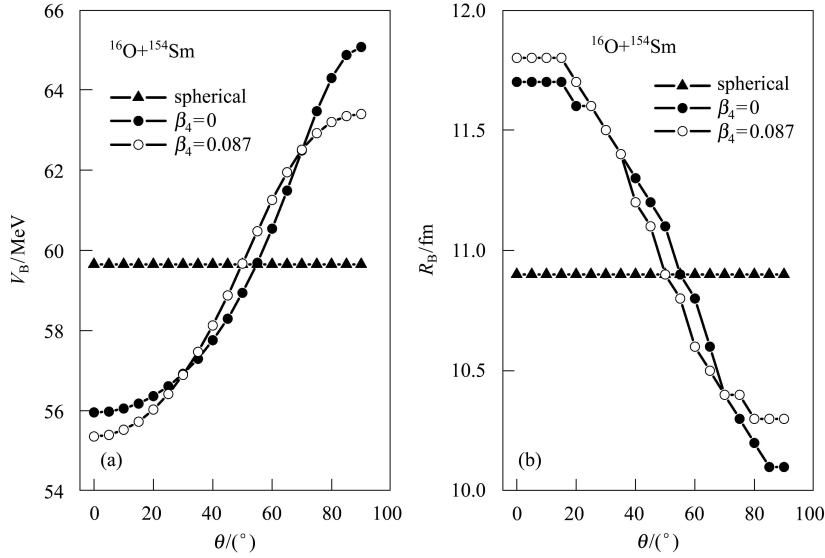
Fig. 4. The barrier heights and positions of the interaction potentials of the system ^{16}O$+^{154}$Sm for $\beta_4=0$, $\beta_4=0.087$ and no deformation, respectively.
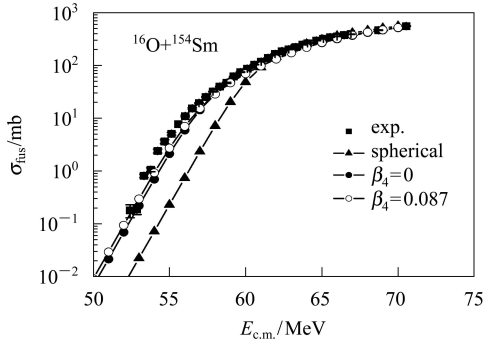
Fig. 5. The fusion cross section of the system ^{16}O$+^{154}$Sm for $\beta_4=0$, $\beta_4=0.087$ and no deformation in comparison with experimental data[1], respectively.

Using Wong's formula[12], we calculate the fusion cross section of the system ^{16}O$+^{154}$Sm.

$$\sigma_f(\theta) = \frac{\hbar\omega R_B^2(\theta)}{2E_{c.m.}} \ln\left[1+\exp\left(\frac{2\pi}{\hbar\omega}(E_{c.m.}-V_B(\theta))\right)\right]. \tag{11}$$

The total fusion cross section is then given by

$$\sigma_f = \frac{1}{4\pi}\int \sigma_f(\theta) 2\pi\sin(\theta)\mathrm{d}\theta. \tag{12}$$

In Fig. 5 we compare our calculations for ^{154}Sm with the experimental data[1]. The calculations have been done for spherical and deformed ^{154}Sm with $\beta_4=0$ and 0.087, respectively. One can see that the integrated fusion cross sections are in rather good agreement with the experimental data, especially at energies around and below the Coulomb barrier, which was the main interest in nuclear physics in the past decades. The fusion cross sections for $\beta_4=0.087$ are larger than those for $\beta_4=0$. It can be seen that a positive hexadecapole deformation increases the fusion cross section relative to that one where only quadrupole deformations have been taken into account. The fusion cross sections around and below the Coulomb barrier are much smaller than the experimental data if the target nucleus ^{154}Sm is treated as undeformed, indicating that the deformation of the target nucleus strongly affects the fusion cross section.

Once the fusion cross section has been calculated, also the barrier distribution can be obtained. The actual distribution of probabilities for finding a fusion barrier at a given center-of-mass energy $E_{\text{c.m.}}$ can be directly extracted from the fusion cross sections σ_{f} by a twofold differentiation of $E_{\text{c.m.}}\sigma$ with respect to the energy:

$$D(E_{\text{c.m.}}) = \frac{\mathrm{d}^2(E_{\text{c.m.}}\sigma)}{\mathrm{d}E_{\text{c.m.}}^2} \ . \tag{13}$$

The barrier distribution of the system ^{16}O+^{154}Sm is shown in Fig. 6, where the target nucleus ^{154}Sm has been treated as spherical and deformed with a hexadecapole parameter β_4=0 and 0.087. The experimental data are from Ref. [13]. From Fig. 6 we find that for the case of no deformation of the target nucleus, the barrier height increases very sharp and the shape of the distribution is very different from the experimental data. However, including the deformation of the target nucleus improves the agreement with the experimental data, especially at low energies. It indicates that the deformation of the target
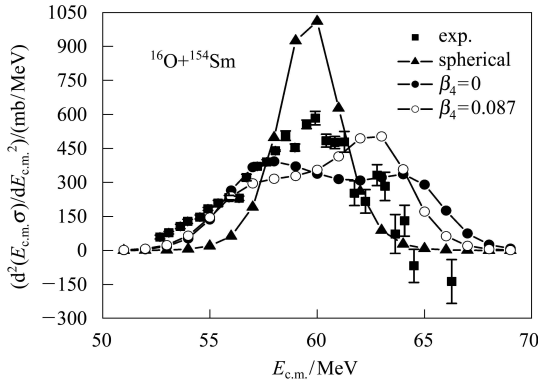
Fig. 6. The barrier distribution of the system ^{16}O+^{154}Sm for β_4=0, β_4=0.087 and no deformation in comparison with experimental data[13].

nucleus has a large effect on the barrier distribution. In particular it can be seen from Fig. 6 that the barrier distribution for the case with β_4=0.087 gives a better agreement with the experimental data than that for β_4=0. It is evident that the inclusion of the hexadecapole deformation can improve the barrier distribution as compared with the case of a pure quadrupole deformation.

In summary, we have applied the double folding model to a pair of nuclei, one deformed, the other spherical. The double folding potentials are obtained numerically by using the truncated multipole expansion method. The system ^{16}O+^{154}Sm was chosen taking the quadrupole and hexadecapole deformations of ^{154}Sm into account. The interaction potentials of the system were calculated at the orientation angles θ=0° and θ=90°. The barrier heights and positions have been obtained for cases with β_4=0, 0.087 and the undeformed target nucleus at different orientation angles. It was shown that the barrier height and position depend strongly on the orientation angles and deformations. Therefore they have also a large effect on the fusion cross section, especially at energies around and below the Coulomb barrier, and they also have a large influence on the barrier distribution. The integrated fusion cross sections agree well with the experimental data and also the barrier distribution reproduces the experimental data quite well. The results of the present work should be meaningful in studies of heavy-ion fusion reactions, where the deformation of the nuclei plays an important role. It is well suited to allow us to reliably explore heavy-ion fusion reactions, especially for sub-barrier fusion processes.

References

1 Leigh J R et al. Phys. Rev. C, 1995, **52**: 3151
2 LIU Z H, BAO J D. Chin. Phys. Lett., 2004, **21**: 1491
3 ZHANG Gao-Long et al. HEP & NP, 2007, **31**: 634 (in Chinese)
4 LU Xi-Ting. Nuclear Physics. Beijing: Atomic Energy Press, 1980. 178 (in Chinese)
5 Satchler G R, Love W G. Phys. Rep., 1979, **55**: 183
6 Gontchar I I, Hinde D J, Dasgupta M, Morton C R, Newton

J O. Phys. Rev. C, 2006, **73**: 034610
7 Rhoades-Brown M J, Oberacker V E, Seiwert M, Greiner W. Z. Phys. A, 1983, **310**: 287
8 XU C, REN Z Z. Phys. Rev. C, 2006, **73**: 041301
9 Chamon L C et al. Phys. Rev. C, 2004, **70**: 014604
10 De Vries H et al. Atomic Data and Nuclear Data Tables., 1987, **36**: 504
11 Cooper T et al. Phys. Rev. C, 1976, **13**: 1083
12 WONG C Y. Phys. Rev. Lett., 1973, **31**: 766
13 WEI J X et al. Phys. Rev. Lett., 1991, **67**: 3368